Chemical Engineering Journal 163 (2010) 382–388

Contents lists available at ScienceDirect

Chemical Engineering Journal

journal homepage: www.elsevier.com/locate/cej

Biosorption of antimony from aqueous solution by lichen (*Physcia tribacia*) biomass

Ozgur Dogan Uluozlu, Ahmet Sarı*, Mustafa Tuzen

Department of Chemistry, Gaziosmanpasa University, Taşlıçiftlik, 60250 Tokat, Turkey

ARTICLE INFO

Article history:
Received 30 June 2010
Received in revised form 5 August 2010
Accepted 6 August 2010

Keywords:
Physcia tribacia
Lichen
Antimony
Biosorption
Equilibrium
Thermodynamics
Kinetics

ABSTRACT

The biosorption characteristics of antimony(III) from aqueous solution using lichen (*Physcia tribacia*) biomass was investigated in terms of equilibrium, thermodynamics and kinetics. Optimum biosorption conditions were determined with respect to pH, biomass concentration, contact time, and temperature. Langmuir, Freundlich and Dubinin–Radushkevich (D–R) isotherm models were applied to the equilibrium data. The maximum Sb(III) sorption capacity of *P. tribacia* was found to be 81.1 mg/g at pH 3, biomass concentration 4 g/L, contact time 30 min, and temperature 20 °C. The calculated mean biosorption energy (10.2 kJ/mol) using D–R model indicated that the biosorption of Sb(III) on the biomass was occurred by chemical ion exchange. The highest desorption efficiency (95%) was achieved using 0.5 M HCl. The biosorption capacity of *P. tribacia* slightly decreased about 10% after ten times of sorption–desorption process. The calculated thermodynamic parameters showed that the biosorption of Sb(III) onto *P. tribacia* biomass was feasible, spontaneous and exothermic, respectively. The experimental data was also examined using the Lagergren's first-order and pseudo-second-order kinetic models. The results revealed that the pseudo-second-order kinetic model provided the best description of the equilibrium data.

1. Introduction

Excessive discharge of toxic metals to environment due to industrialization has created great global concern in recent years. Antimony is raised much concern in terms of toxicological and environmental. It has been extensively used in lead alloys, battery grids, bearing metal, cable sheathing, plumber's solder, pewter, ammunition, sheet and pipe. Among the most important uses of antimony in non-metal products are textiles, paints and lacquers, rubber compounds, ceramic enamels, glass and pottery abrasives phosphorus (a beryllium replacement) [1]. Because of its classification of antimony as a toxic environmental pollutant and with implication in cancer development [2–5], its compounds are considered to be pollutants of priority interest by the United States Environmental Protection Agency (USEPA) [6] and the European Union (EU) [7].

Antimony is regulated as a drinking water contaminant because it can cause health effects, such as nausea, vomiting, and diarrhea, when exposure exceeds the maximum contaminant level for relatively short periods. Long-term exposure can lead to increased blood cholesterol and decreased blood sugar. Although USEPA has not identified antimony as a human carcinogen in water due to lack of studies, research shows that antimony and arsenic, a proven carcinogen, are similarly toxic [8]. The World Health Organization (WHO) guidelines the antimony concentration as 0.005 mg/L in drinking waters [9]. The toxicological effects of antimony depend on its chemical form and oxidation state [10]. The most favored form of antimony in water is the pentavalent antimonate oxoanion [$Sb(OH)_6^-$], while its other common inorganic form is antimonite [$Sb(OH)_3$] [10]. The Sb(III) form is 10 times more toxic than Sb(V) form [11].

Because of the toxicological effects of antimony, its monitoring and subsequent removal from aqueous solution has been compulsory [12]. A number of methods have been used for the removal of antimony. These methods can be ordered as reduction and chemical precipitation [13,14], solvent extraction [15], ion exchange [16] and adsorption [17–22]. These methods have several disadvantages. Chemical precipitation leads to the production of toxic sludge. Due to the economics of dealing with large volumes of liquids and of solvent losses, solvent extraction is limited to streams containing more than 1 g/L of the targeted heavy metal. Application of the ion-exchange process is rather expensive due to the cost of synthetic ion-exchange resins. Adsorption method is more effective in reducing heavy metal concentration [23–25]. However, adsorbents must have a large surface area and high polarity between the attractive forces on the adsorbent surface and adsorbate. Adsorption is also sometimes found to be expensive and time consuming.

Alternative methods of metal removal and recovery based on biological materials have been considered. Biologicalmaterials are

* Corresponding author. Tel.: +90 356 2521616; fax: +90 356 2521585.
E-mail address: asari@gop.edu.tr (A. Sarı).

1385-8947/$ – see front matter © 2010 Elsevier B.V. All rights reserved.
doi:10.1016/j.cej.2010.08.022

sources of abundant low-cost biomasses and there are no environmental or technical reasons which limit the use of these materials in the preparation of biosorbents [26–30].

Lichens are composite plants composed of fungi and algae [31]. They are considered as indicator of environmental quality due to their accumulating ability of a variety of contaminants, particularly heavy metals [32–36] and radionuclides [37]. The *Physcia tribacia* is a biomass in lichen class and growing mainly on rocks in open situations and widely distributed but not common in northern and southern temperate regions. According to authors' survey, there is no extensive study on the biosorptive removal of antimony from aqueous solutions using *P. tribacia* biomass in literature. In addition, this material was chosen as novel biosorbent in this study due to being of its naturally abundant, renewable and thus cost-effective biomass.

The aim of this work is to investigate the biosorption potential of *P. tribacia* biomass in the removal of Sb(III) from aqueous solution. The Langmuir and Freundlich and D–R isotherm models were used to describe equilibrium isotherms. The desorption of Sb(III) from *P. tribacia* was also studied using 0.5 M HCl and 0.5 M HNO_3 solutions. The biosorption kinetics was examined using the Lagergren's pseudo-first-order and pseudo-second-order models. In addition, the biosorption of Sb(III) onto *P. tribacia* was evaluated from point of thermodynamics.

2. Experimental

2.1. Biomass preparation

The lichen (*P. tribacia*) samples were collected from the Efirli Village in Perşembe District of Ordu Province, Turkey. The samples were washed with deionized water to remove extraneous materials and salts. They were then dried in an oven at 60 °C for 48 h until no variation in the sample weight observed. The dried lichen biomass was chopped, sieved and the particles with an average of 0.5 mm were used for biosorption experiments.

2.2. Structural characterization by infrared spectroscopy analysis

The FT-IR spectroscopy method was used to obtain information on the nature of probable interactions between the functional groups on the surface of the biomass and antimony ions. A sample of biomass is mixed with dry KBr in a ratio of 1 mg/250 mg. The mixture is ground and compressed. The FT-IR spectra of unloaded biomass and Sb(III)-loaded biomass were taken at 400–4000 cm^{-1} wave number range using a FT-IR spectrometer (JASCO-430 model, Japan).

2.3. Equipments

A pH meter (Sartorius pp-15 Model glass-electrode) was prepared for measuring pH values in the aqueous phase. The antimony concentration was determined using AAS system (Perkin Elmer Analyst 700 mode, l Norwalk, CT, USA) equipped with MHS 15 HGAAS system. A hallow cathode lamp operating at 15 mA was used and a spectral bandwidth of 0.7 nm was selected to isolate the 231.2 nm antimony line. $NaBH_4$ (1.5%) (w/v) in NaOH (0.5%) (w/v) was used as reducing agent. The analytical measurement was based on peak height. Reading time and argon flow rate was selected as 20 s and 70 mL min^{-1}. To ensure the accuracy, reliability and reproducibility of the collected data, the measurements were carried out in duplicated and the average values are presented. The error bars were also shown in the presentation of the results.

2.4. Batch biosorption procedure

Sb(III) standard solution (1000 mg/L) was prepared from $SbCl_3$ (E. Merck, Darmstadt, Germany). Sodium phosphate buffer, ammonium acetate buffer and ammonium chloride buffer was used for pH arrangement of the aqueous solutions. The biomass was then added and content in the flask was shaken for desired contact time on an electrically thermostatic reciprocating shaker (Selecta multimatic-55 model, Spain) at 120 rpm. The time required for reaching the equilibrium condition was estimated by drawing samples at regular intervals of time until equilibrium was reached. The content of the flask was filtered through filter paper and the filtrate was analyzed for antimony concentration using AAS system.

The batch biosorption procedure mentioned above were repeated at the following experimental parameters: the contact time 5–90 min, pH 2–10, initial metal concentration 10–400 mg/L, the biomass concentration 1–20 g/L and the temperature 20–50 °C. The percent biosorption of Sb(III) was calculated as follows:

$$\text{Biosorption}\,(\%) = \frac{(C_i - C_f)}{C_i} \times 100 \quad (1)$$

where C_i (mg/L) and C_f (mg/L) are the initial and final Sb(III) concentrations, respectively.

2.5. Biosorption isotherm models

A biosorption isotherm is used to express the surface properties and affinity of the biosorbent. It can also be used to compare the biosorptive capacities of the biosorbent for different pollutants. In this study, the three isotherm models, the Langmuir, Freundlich and Dubinin–Radushkevich (D–R) were applied to the equilibrium data.

A basic assumption of the Langmuir theory is that sorption takes place at specific homogeneous sites within the sorbent. This model can be written in non-linear form [38].

$$q_e = \frac{q_m K_L C_e}{1 + K_L C_e} \quad (2)$$

where q_e is the equilibrium metal ion concentration on sorbent (mg/g), C_e is the equilibrium metal ion concentration in the solution (mg/L), q_m is the monolayer biosorption capacity of the sorbent (mg/g), and K_L is the Langmuir biosorption constant (L/mg) related with the free energy of biosorption. Non-linear regression analysis was carried out in SigmaPlot software (SigmaPlot 2001, SPSS Inc., USA) in order to determine K_L and q_m values.

The Freundlich model assumes a heterogeneous adsorption surface and active sites with different energy. The Freundlich model [39] is

$$q_e = K_f C_e^{1/n} \quad (3)$$

where K_f is a constant relating the biosorption capacity and $1/n$ is an empirical parameter relating the biosorption intensity, which varies with the heterogeneity of the material.

The D–R isotherm model was also applied to the equilibrium data to determine the nature of biosorption process as physical or chemical. The linear presentation of the D–R isotherm equation [40] is expressed by

$$\ln\ q_e = \ln\ q_m - \beta\varepsilon^2 \quad (4)$$

where q_e is the amount of metal ions sorbed on per unit weight of biomass (mol/L), q_m is the maximum biosorption capacity (mol/g), β is the activity coefficient related to biosorption mean free energy (mol^2/J^2) and ε is the Polanyi potential ($\varepsilon = RT\ln(1 + 1/C_e)$). The biosorption mean free energy (E; kJ/mol) was calculated using the

following equation

$$E = \frac{1}{\sqrt{-2\beta}} \quad (5)$$

The E (kJ/mol) value gives information about sorption mechanism, physical or chemical. If it lies between 8 and 16 kJ/mol, the sorption process is occurred chemically. If E <8 kJ/mol, it is occurred physically [41].

2.6. Biosorption kinetic models

The prediction of biosorption rate is important for designing batch biosorption systems. Two kinetic models, Lagergren's pseudo-first-order and pseudo-second-order models were tested to clarify the biosorption kinetics of Sb(III) by *P. tribacia* biomass. The linear form of the pseudo-first-order rate equation by Lagergren [42] is given as

$$\ln(q_e - q_t) = \ln\ q_e - k_1 t \quad (6)$$

where q_t and q_e (mg/g) are the amounts of the metal ions biosorbed at equilibrium (mg/g) and t (min), respectively and k_1 is the rate constant of the equation (min^{-1}).

Experimental data were also tested by the pseudo-second-order kinetic model which is given in the following form [43]:

$$\frac{t}{q_t} = \frac{1}{k_2 q_e^2} + \left(\frac{1}{q_e}\right) t \quad (7)$$

where k_2 (g/mg min) is the rate constant of the second-order equation, q_t (mg/g) is the amount of biosorption time t (min) and q_e is the amount of biosorption equilibrium (mg/g).

2.7. Thermodynamics of biosorption

The thermodynamic parameters including the change in free energy (ΔG°), enthalpy (ΔH°) and entropy (ΔS°) were calculated from following equations

$$\Delta G^\circ = -RT\ \ln K_D \quad (8)$$

where, R is the universal gas constant (8.314 J/mol K), T is temperature (K) and K_D (q_e/C_e) is the distribution coefficient [44].

The enthalpy (ΔH°) and entropy (ΔS°) parameters were estimated from the following equation

$$\ln\ K_D = \frac{\Delta S^\circ}{R} - \frac{\Delta H^\circ}{RT} \quad (9)$$

2.8. Desorption procedure

The Sb(III) ions sorbed onto *P. tribacia* biomass were desorbed using 10 mL of 0.5 M HCl and 10 mL of 0.5 M HNO_3, separately. Antimony content of the solution was determined by HGAAS. In order to use the biomass for the next experiment, it was washed with excess of 0.5 M HCl solution and distilled water, sequentially.

3. Results and discussion

3.1. Effect of pH

Solution pH affects the metal binding sites of the sorbent and the metal ion chemistry in aqueous solution [45,46]. The effect of pH on metal biosorption by lichen biomass was studied by different authors [32,34,47].

The effect of pH on the biosorption of Sb(III) onto *P. tribacia* biomass was studied at pH 2–10, metal concentration 10 mg/L, biomass concentration 4 g/L, and temperature 20 °C. The results were presented in Fig. 1. In aqueous solution Sb(III) is available as $[SbO]^+$ and $[Sb(OH)_2]^+$ species at pH < 3. $[HSbO_2]$ and $[Sb(OH)_3]$ species are predominant at pH 3–10 and $[SbO_2]^-$ specie is existing in aqueous solution at pH > 10 [12,48]. In the present work, the Sb(III) sorption was found to be 96–85% at pH 3–6. The highest sorption (96%) was achieved at pH 3 while the lowest biosorption yield was 73% at pH 2 and 53% after pH 8. Therefore, pH 3 was selected as optimum pH for further experiments. At pH < 3, the low biosorption yield can be due to the fact that the competition for the binding to the cell of the biomass between the hydronium ions and predominant cationic antimony species, $[SbO]^+$. When the pH values increased from 3 to 8, biosorbent surface was more negatively charged and the deprotonated functional groups of the biomass had suitable position for binding antimony ions. Decrease in biosorption at higher pH (pH > 8) can be attributed to the competition for the sorption sites between hydroxyl ions and predominant the anionic antimony species, $[SbO_2]^-$. Similar results have also been reported for the sorption of antimony on rice husks [1], metal-loaded saponified orange waste [12], goethite (α-FeOOH) [48] and activated alumina [49].

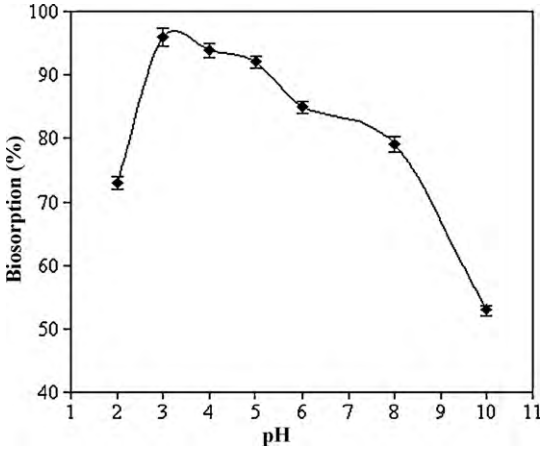

Fig. 1. Effect of pH on the biosorption of Sb(III) by *P. tribacia* biomass (antimony concentration:10 mg/L; temperature: 20 °C).

3.2. Effect of biomass concentration

The biomass concentration is an important parameter in terms of the determination of the capacity of biosorbent for any initial concentration [50]. The biosorption efficiency as a function of biomass concentration was investigated at other experimental conditions, metal concentration 10 mg/L, pH 3 and temperature 20 °C. The results are shown in Fig. 2. The antimony biosorption steeply increases with the biomass concentration up to 4 g/L. Increase in the biosorption percent with increase in biomass concentration was attributed to the availability of more sorption sites. At very low biomass concentration, the biosorbent surface becomes saturated with the metal ions and the residual metal ion concentration in the solution is large. However, a significant increase in the biosorption percent was not observed when the biomass concentration was increased over 4 g/L. The biosorption yield was 95% for the biomass concentration 4 g/L as it was found to be 97% for the biomass concentration 20 g/L. Therefore, the biomass concentration 4 g/L was selected as optimum for further experiments.

3.3. Effects of contact time and temperature

Contact time is one of the most important parameters for successful utility of biomass in practical and rapid sorption applications [51]. The effect of the contact time on the biosorption of antimony (metal concentration 10 mg/L, biomass concentration

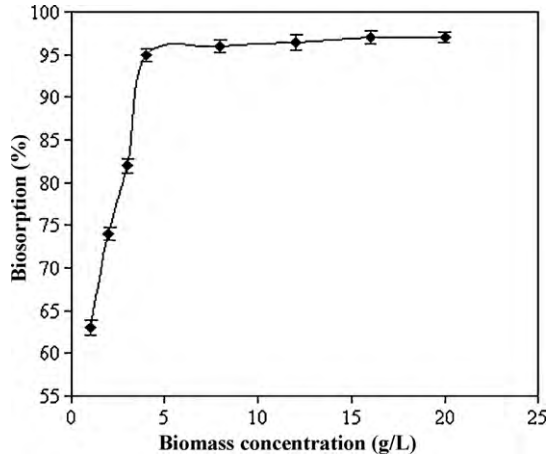

Fig. 2. Effect of biomass dosage on the biosorption of Sb(III) by *P. tribacia* biomass (antimony concentration:10 mg/L; pH: 3; temperature: 20 °C).

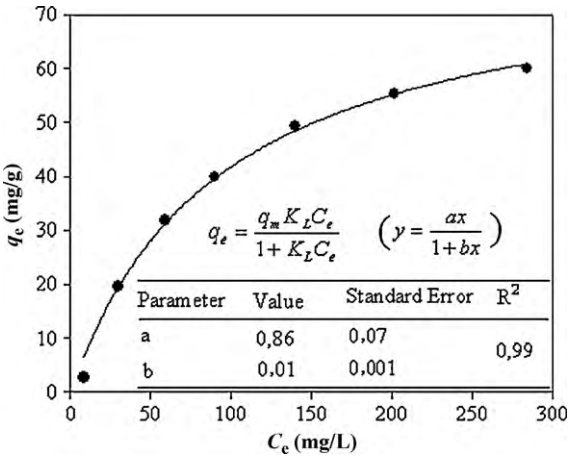

Fig. 4. Langmuir isotherm plots for the biosorption of Sb(III) by *P. tribacia* biomass (biomass concentration: 4 g/L; contact time: 30 min; pH: 3; temperature: 20 °C).

4 g/L and pH 3 and the results were shown in Fig. 3. The biosorption of antimony is fast and the equilibrium was achieved by 30 min of contact time.

Temperature of the medium is also an effective parameter on biosorption efficiency. Thus, the biosorption experiments were carried out at the temperature range 20–50 °C. As seen from Fig. 3, the biosorption percent decreased from 96% to 80% as temperature was increased from 20 to 50 °C. These results indicated the exothermic nature of antimony biosorption onto *P. tribacia* biomass. The decreasing in biosorption efficiency may be attributed to the following reasons: the relative increase in the escaping tendency of the antimony ions from the solid phase to the bulk phase; deactivating the biosorbent surface or destructing some active sites on the biosorbent surface due to bond ruptures [52] or the weakness of biosorptive forces between the active sites of the sorbents and the sorbate species and also between the adjacent molecules of sorbed phase [53]. The results are in agreement with the point of view of thermodynamics.

3.4. Biosorption isotherms

Fig. 4 indicates the non-linear Langmuir isotherm plot and the standard error in the determination of the parameters. As seen from the figure, the coefficient of determination (R^2) was found to be 0.99. This result indicates that the biosorption of the Sb(III) onto *P. tribacia* biomass fitted well the Langmuir model. From this model, the maximum biosorption capacity (q_m) of *P. tribacia* biomass was found to be 81.1 mg/g. The K_L value was found as 0.01 L/mg. In addition, Table 1 presents the comparison of biosorption capacity of *P. tribacia* for antimony with that of various sorbents reported in literature [12,21,48,54]. As seen from this table, the sorption capacity of *P. tribacia* biomass for antimony is higher than that of the majority of different sorbents. Therefore, it can be concluded that the *P. tribacia* biomass has important potential for the removal of antimony from aqueous solution.

Table 1
Comparison of sorption capacity of *P. tribacia* biomass Sb(III) with that of different sorbents.

Biosorbent	Sorption capacity (mg/g)	Reference
Zr(IV)-loaded SOW	114.5	[12]
Fe(III)-loaded SOW	136.4	[12]
Chemically bonded adsorbent	21.9	[21]
Goethite (α-FeOOH)	61.2 (average value)	[48]
Hydrous oxide of Mn	17.1	[54]
Hydrous oxide of Fe	12.2	[54]
Physcia tribacia	81.1	Present study

Fig. 5 indicates the non-linear Freundlich isotherm plot and the standard error in the determination of the parameters. The K_f and $1/n$ values were found using non-linear regression analy-

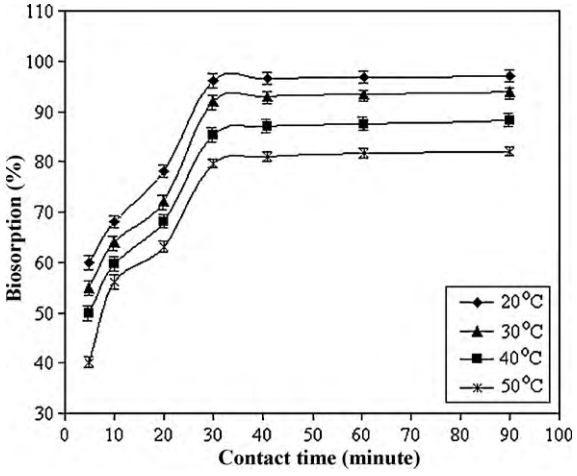

Fig. 3. Effect of contact time and temperature on the biosorption of Sb(III) by *P. tribacia* biomass (antimony concentration:10 mg/L; biomass concentration:4 g/L; pH: 3).

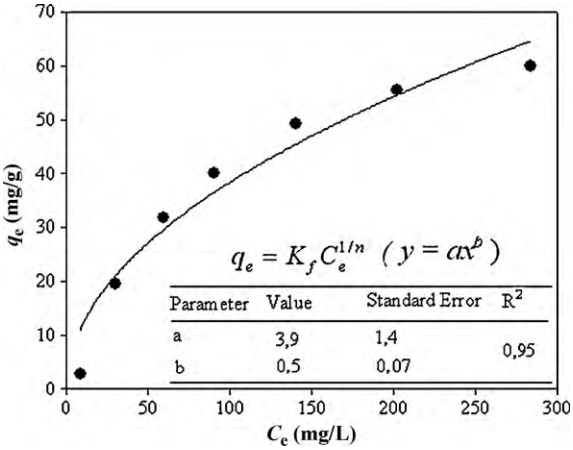

Fig. 5. Freundlich isotherm plots for the biosorption of Sb(III) by *P. tribacia* biomass (biomass concentration: 4 g/L; contact time: 30 min; pH: 3; temperature: 20 °C).

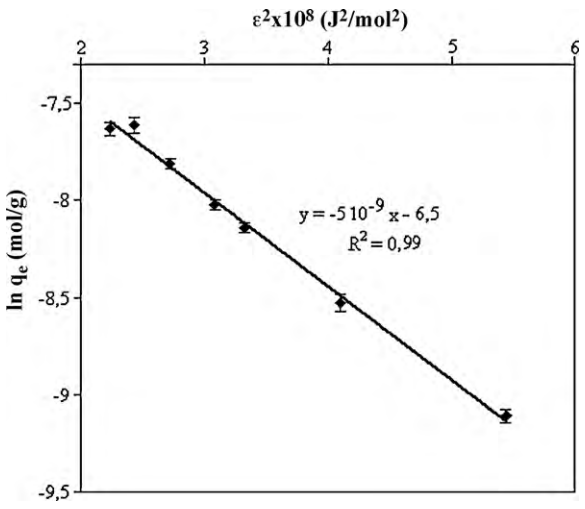

Fig. 6. D-R isotherm plots for the biosorption of Sb(III) by *P. tribacia* biomass (biomass concentration: 4 g/L; contact time: 30 min; pH:3; temperature: 20 °C).

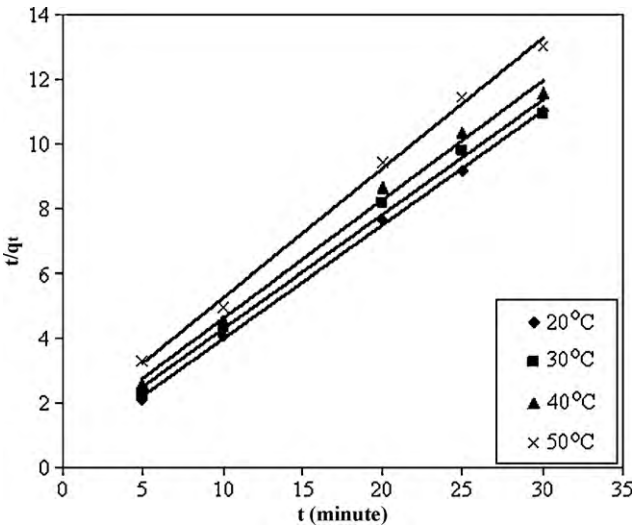

Fig. 8. Pseudo-second-order kinetic plots at different temperatures (metal concentration: 10 mg/L; pH: 3; biomass concentration: 4 g/L).

sis (SigmaPlot software, SigmaPlot 2001, SPSS Inc., USA). From the plot, K_f and $1/n$ values were found to be 3.9 and 0.5, respectively. The $1/n$ value were between 0 and 1 indicating that the biosorption of Sb(III) using *P. tribacia* biomass was favorable at studied conditions. The R^2 value was found to be 0.95. This results indicated that the Freundlich model is not sufficient to describe the relationship between the amount of sorbed Sb(III) onto the biomass and its equilibrium concentration in the solution.

The D–R isotherm model well fitted the equilibrium data since the R^2 value was found to be 0.99 (Fig. 6). The q_m value was found using the intercept of the plot to be 15×10^{-4} mol/g. The mean free energy value was also calculated to be 10.2 kJ/mol. It means that that the biosorption of Sb(III) onto *P. tribacia* biomass was carried out by chemical ion-exchange mechanism.

3.5. Desorption efficiency

Desorption of Sb(III) from the *P. tribacia* biomass was studied separately using 0.5 M HCl (10 mL) and 0.5 M HNO_3 (10 mL). The highest desorption efficiency was achieved as about 95% and 78% using 0.5 M HCl and 0.5 M HNO_3, respectively. As also seen in Fig. 7, the high stability of *P. tribacia* biomass permitted 10 times of biosorption–desorption process along the studies with a decrease about 20% in biosorption efficiency of Sb(III). These results mean that *P. tribacia* biomass was good biosorbent with respect to the biosorption performance after a large number of sorption–desorption cycling.

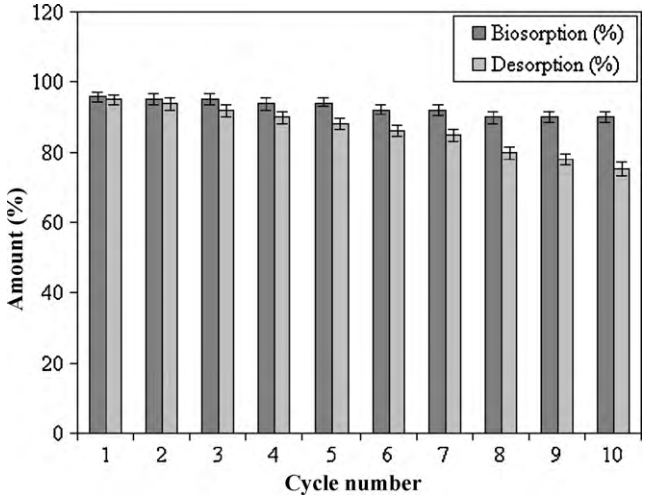

Fig. 7. Biosorption–desorption efficiency with cycle number (biomass concentration: 4 g/L; contact time: 30 min; temperature: 20 °C).

3.6. Biosorption kinetics

Based on Eq. (6) the biosorption rate constants (k_1) can be determined experimentally by plotting of $\ln(q_e - q_t)$ vs. t. As seen from the R^2 and $q_{e,exp}$ values in Table 2, the pseudo-first-order model is not fitting for the biosorption of Sb(III) onto *P. tribacia* biomass.

The pseudo-second-order kinetic model is more probable to predict kinetic behavior of biosorption with chemical sorption being the rate-controlling step [55]. The linear plots of t/q_t vs. t for the pseudo-second-order model for the biosorption of Sb(III) by *P. tribacia* at 20–50 °C were shown in Fig. 8. As seen from Table 2, the R^2 values are in range of 0.992–0.996 and the theoretical $q_{e2,cal}$ values were closer to the experimental $q_{e,exp}$ values. Based on these results, it can be concluded that the pseudo-second-order kinetic model provided a good correlation for the biosorption of Sb(III) by *P. tribacia* in contrast to the pseudo-first-order model.

3.7. Thermodynamics parameters of biosorption

According to Eq. (9), the ΔH° and ΔS° parameters can be calculated from the slope and intercept of the plot of $\ln K_D$ vs. $1/T$ yields, respectively (Fig. 9). Gibbs free energy change (ΔG°) was calculated to be −18.9, −18.1, −16.5, and −15.3 kJ/mol for 20, 30, 40, and 50 °C, respectively. The negative ΔG° values indicate the spontaneous nature of the biosorption. The negative ΔH° (−55.7 kJ/mol) means that the biosorption of process was carried out as exothermic at 20–50 °C. Furthermore, the negative ΔS° (−124.9 kJ/mol K) reveals the decreased randomness at the solid–solution interface during the fixation of the antimony ion on the active sites of the biosorbent.

3.8. FT-IR analysis

The FT-IR results are presented in Fig. 10. The broad and strong bands at 3300–3580 cm^{-1} represent the bounded hydroxyl (−OH) groups of the lichen biomass. The peaks at 2335 and 2362 cm^{-1} signify the stretching vibrations of $-NH_2^+$, $-NH^+$ and

Table 2
Kinetic parameters obtained from pseudo-first-order and pseudo-second-order at different temperatures.

Pseudo-first-order					Pseudo-second-order		
Temperature (°C)	$q_{e,exp}$ (mg/g)	k_1 (l/min)	$q_{e1,cal}$ (mg/g)	R^2	k_2 (g/mg min)	$q_{e2,cal}$ (mg/g)	R^2
20	3.2	0.15	1.7	0.87	0.15	3.2	0.99
30	2.9	0.13	1.5	0.87	0.14	3.1	0.99
40	2.8	0.74	1.4	0.88	0.13	2.9	0.99
50	2.5	0.36	1.3	0.89	0.11	2.7	0.99

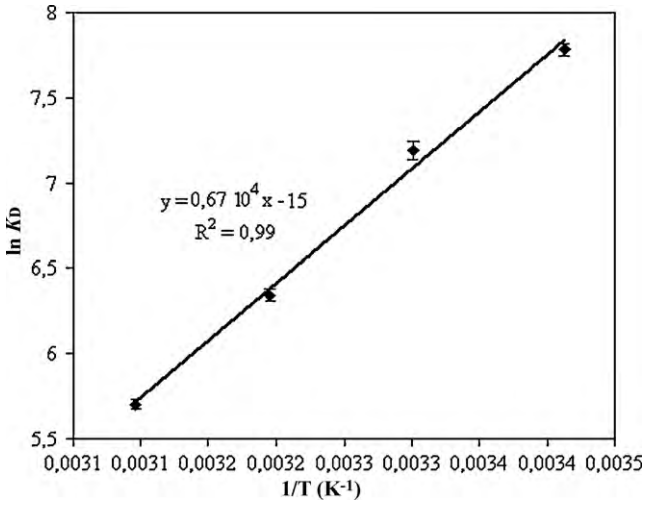

Fig. 9. Plot of $\ln K_D$ vs. $1/T$ for the estimation of thermodynamic parameters for biosorption of Sb(III) by *P. tribacia* biomass (pH: 3; biomass concentration: 4 g/L; contact time: 30 min).

–NH groups of the biomass. The bands peaks at 1643, 1517 and 1423 cm^{-1} may be attributed to asymmetric and symmetric stretching vibration of carboxyl (–C=O) groups. The bands observed at 1049 and 1105 cm^{-1} were assigned to C–O stretching of alcohols and carboxylic acids. Some bands in the fingerprint region could be attributed to the phosphate groups. After Sb(III) biosorption, the stretching vibration bands of hydroxyl were shifted to 3290–3588 cm^{-1} for Sb(III)-loaded biomass. The stretching vibration bands of amide groups were shifted to 2329 and 2358 cm^{-1}. The asymmetric and symmetric stretching vibration bands of carboxyl groups were shifted to 1648, 1512 and 1419 cm^{-1}. The bands assigned to C–O stretching were also shifted to 1108 and 1045 cm^{-1}. These results indicated that the chemical interactions as ion exchange between the metal ions and the hydrogen atoms of carboxyl, hydroxyl, and amide groups of the biomass were mainly involved in the biosorption. The similar FT-IR results were reported for the biosorption of Hg(II) by *Xanthoparmelia conspersa* [33], Pb(II) and Ni(II) by *Cladonia furcata* [35] and Pb(II) and Cr(III) by *Parmelina tiliaceae* as lichen biomasses [36].

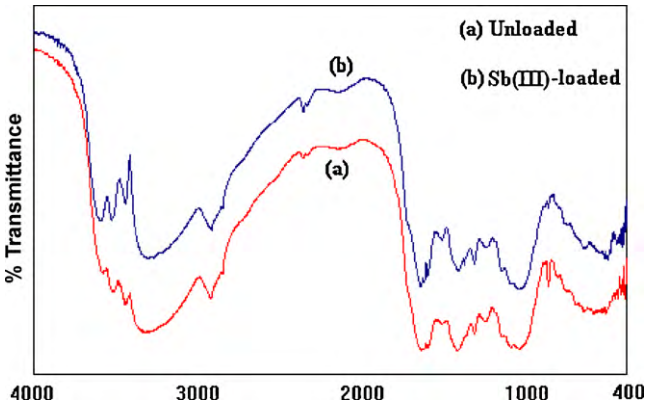

Fig. 10. FT-IR spectrum of unloaded and Sb(III)-loaded biomass.

4. Conclusions

In this study, the biosorption characteristics of antimony(III) from aqueous solution using lichen (*P. tribacia*) biomass was investigated in terms of equilibrium, thermodynamics and kinetics. The experimental parameters, pH of solution, biomass concentration, contact time, and temperature, were effective on the biosorption of Sb(III) using *P. tribacia* biomass. The maximum biosorption capacity of *P. tribacia* biomass was found to be 81.1 mg/g at pH 3, contact time of 30 min, biomass concentration of 4 g/L, and temperature of 20 °C. The calculated mean free energy (10.2 kJ/mol) from the D–R model indicated that the biosorption of Sb(III) using *P. tribacia* biomass was taken place by chemical ion exchange. The highest desorption efficiency (95%) was achieved using 0.5 M HCl. The biosorption efficiency of *P. tribacia* slightly decreased about 20% even after 10 times of adsorption-elution process. The calculated thermodynamic parameters showed that the biosorption of Sb(III) onto *P. tribacia* biomass was feasible, spontaneous and exothermic under studied experimental conditions. Furthermore, the experimental data were fitted to the Lagergren's first-order and pseudo-second-order kinetic models. The kinetic results revealed that the pseudo-second-order model was the best kinetic model for the description of the biosorption mechanism. Based on all results, it can be also concluded that the *P. tribacia* biomass can be evaluated as an alternative biosorbent for the treatment of wastewater containing Sb(III) ions, due to its being low-cost biomass and having a considerable high sorption capacity.

Acknowledgement

The authors are grateful for the financial support of the Unit of the Scientific Research Projects of Gaziosmanpaşa University. The authors also would like to thank Dr. Kadir Kınalıoğlu for identification of the lichen.

References

[1] N. Khalid, S. Ahmad, A. Toheed, J. Ahmed, Potential of rice husks for antimony removal, Appl. Radiat. Isot. 52 (2000) 31–38.
[2] X. Guo, Z. Wu, M. He, Removal of antimony(V) and antimony(III) from drinking water by coagulation–flocculation–sedimentation (CFS), Water Res. 43 (2009) 4327–4335.
[3] N. Gurnani, A. Sharma, G. Tulukder, Effects of antimony on cellular systems in animals: a review, Nucleus 37 (1994) 71–96.
[4] T. Gebel, Arsenic and antimony: comparative approach on mechanistic toxicology, Chem. Biol. Interact. 107 (1997) 131–144.
[5] K. Oorts, E. Smolders, F. Degryse, J. Buekers, G. Casco, G. Cornelis, J. Mertens, Solubility and toxicity of antimony trioxide (Sb_2O_3) in soil, Environ. Sci. Technol. 42 (2008) 4378–4383.
[6] USEPA, Water Related Fate of the 129 Priority Pollutants, vol. 1, USEPA, Washington, DC, 1979, Doc. 745-R-00-007.
[7] CEC (Council of the European Communities), Council Directive 76/substances discharged into aquatic environment of the community, Off. J. L 129 (1976) 23–29.
[8] P. Westerhoff, P. Prapaipong, E. Sho ckb, A. Hillaireau, Antimony leaching from polyethylene terephthalate (PET) plastic used for bottled drinking water, Water Res. 42 (2008) 551–556.

[9] World Health Organization (WHO), Health criteria and other supporting information, in: Guidelines for Drinking-Water Quality, 2, 2nd ed., 1996, pp. 940–949.
[10] M. Fiella, N. Belzile, M.-C. Lett, Antimony in the environment: a review focused on natural waters. III. Microbiota relevant interaction, Earth-Sci. Rev. 80 (2007) 195–217.
[11] P. Smichowski, Y. Madrid, C. Camara, Analytical methods for antimony speciation in waters at trace and ultratrace levels. A review, Fresenius J. Anal. Chem. 360 (1998) 623–629.
[12] B.K. Biswas, J. Inoue, H. Kawakita, K. Ohto, K. Inoue, Effective removal and recovery of antimony using metal-loaded saponified orange waste, J. Hazard. Mater. 172 (2009) 721–728.
[13] K. Gannon, D.J. Wilson, Removal of antimony from aqueous solutions, Sep. Sci. Technol. 21 (1986) 475–493.
[14] S.E. Ghazy, Removal of cadmium, lead, mercury, tin, antimony, and arsenic from drinking and seawaters by colloid precipitate flotation, Sep. Sci. Technol. 30 (1995) 933–947.
[15] W.M. Mok, C.M. Wai, Distribution and mobilization of arsenic and antimony species in the Coeur D'Alene River, Idaho, Environ. Sci. Technol. 24 (1990) 102–108.
[16] R. Guin, S.K. Das, S.K. Saha, The anion exchange behavior of Te and Sb, J. Radioanal. Nucl. Chem. Art. 230 (1998) 269–271.
[17] N.V. Deorkar, L.L. Tavlarides, A chemically bonded adsorbent for separation of antimony, copper and lead, Hydrometallurgy 46 (1997) 121–135.
[18] A Kathrinleuz, H. Mönch, C.A. Johnson, Sorption of Sb(III) and Sb(V) to goethite: influence on Sb(III) oxidation and mobilization, Environ. Sci. Technol. 40 (2006) 7277–7282.
[19] M.A.M.M. Khraisheh, Y.S. Al-Degs, W.A.M. Mcminn, Remediation of wastewater containing heavy metals using raw and modified diatomite, Chem. Eng. J. 99 (2004) 177–184.
[20] M.A. Al-Ghouti, M.A.M.M. Khraisheh, M. Tutuji, Flow injection potentiometric stripping analysis for study of adsorption of heavy metal ions onto modified diatomite, Chem. Eng. J. 104 (2004) 83–91.
[21] A. Sarı, D. Cıtak, M. Tuzen, Equilibrium, thermodynamic and kinetic studies on adsorption of Sb(III) from aqueous solution using low-cost natural diatomite, Chem. Eng. J. 162 (2010) 521–527.
[22] S.M. Hasany, M.H. Chaudhary, Sorption potential of haro river sand for the removal of antimony from acidic aqueous solution, Appl. Radiat. Isot. 47 (1996) 467–471.
[23] S. Imai, M. Muroi, A. Hamaguchi, R. Matsushita, M. Koyama, Preparation of dithiocarbamatecellulose derivatives and their adsorption properties for trace elements, Anal. Chim. Acta 113 (1980) 139–147.
[24] J. Li, J. Hu, G. Sheng, G. Zhao, Q. Huang, Effect of pH, ionic strength, foreign ions and temperature on the adsorption of Cu(II) from aqueous solution to GMZ bentonite, Colloid Surf. A: Physicochem. Eng. Aspects 349 (2009) 195–201.
[25] K.G. Bhattacharyya, S. Sen Gupta, Influence of acid activation on adsorption of Ni(II) and Cu(II) on kaolinite and montmorillonite: kinetic and thermodynamic study, Chem. Eng. J. 136 (2008) 1–13.
[26] E. Demirbas, N. Dizge, M.T. Sulak, M. Kobya, Adsorption kinetics and equilibrium of copper from aqueous solutions using hazelnut shell activated carbon, Chem. Eng. J. 148 (2009) 480–487.
[27] V.C. Srivastava, I.D. Mall, I.M. Mishra, Adsorption thermodynamics and isosteric heat of adsorption of toxic metal ions onto bagasse fly ash (BFA) and rice husk ash (RHA), Chem. Eng. J. 132 (2007) 267–278.
[28] T. Perez-Corona, Y. Madrid, C. Camara, Evaluation of antimony selective uptake of selenium (Se(IV) and Se(VI)) and (Sb(III) and Sb(V)) species by baker's yeast cells, *(Saccharomyces cerevisiae)*, Anal. Chim. Acta 345 (1997) 249–255.
[29] J. Tomko, M. Bačkor, M. Štofko, Biosorption of heavy metals by dry fungi biomass, Acta Metall. Slovaca 12 (2006) 447–451.
[30] Y. Madrid, M.E. Barrio-Cordoba, C. Cámara, Biosorption of antimony and chromium species by *Spirulina platensis* and *Phaseolus*. Applications to bioextract antimony and chromium from natural and industrial waters, Analyst 123 (1998) 1593–1598.
[31] X. Lin, Y.J. Cai, Z.X. Li, Q. Chen, Z.L. Liu, R. Wang, Structure determination, apoptosis induction, and telomerase inhibition of CFP-2, a novel lichenin from *Cladonia furcata*, Biochim. Biophys. Acta 1622 (2003) 99–108.
[32] E. Nieboer, K.J. Puckett, B. Grace, The uptake of nickel by *Umbilicaria muhlenbergii*: a physiochemical process, Can. J. Bot. 54 (1976) 724–733.
[33] M. Tuzen, A. Sari, D. Mendil, M. Soylak, Biosorptive removal of mercury(II) from aqueous solution using lichen (*Xanthoparmelia conspersa*) biomass: kinetic and equilibrium studies, J. Hazard. Mater. 169 (2009) 263–270.
[34] F. Ekmekyapar, A. Aslan, Y.K. Bayhan, A. Cakici, Biosorption of copper(II) by nonliving lichen biomass of *Cladonia rangiformis* hoffm, J. Hazard. Mater. 137 (2006) 293–298.
[35] A. Sarı, M. Tuzen, O.D. Uluozlu, M. Soylak, Biosorption of Pb(II) and Ni(II) from aqueous solution by lichen (*Cladonia furcata*) biomass, Biochem. Eng. J. 37 (2007) 151–158.
[36] O.D. Uluozlu, A. Sari, M. Tuzen, M. Soylak, Biosorption of Pb(II) and Cr(III) from aqueous solution by lichen (*Parmelina tiliaceae*) biomass, Bioresour. Technol. 99 (2008) 2972–3298.
[37] T.H. Nash, V. Wirth, Lichens, bryophytes and air quality, Bibl. Lichenol. 30 (1988) 1–298.
[38] M. Ghaedi, F. Ahmadi, Z. Tavakoli, M. Montazerozohori, A. Khanmohammadi, M. Soylak, Three modified activated carbons by different ligands for the solid phase extraction of copper and lead, J. Hazard. Mater. 152 (2008) 1248–1255.
[39] M. Ghaedi, F. Ahmadi, M. Soylak, Simultaneous preconcentration of copper, nickel, cobalt and lead ions prior to their flame atomic absorption spectrometric determination, Annali di Chimica 97 (2007) 277–285.
[40] G Akcin, O. Saltabas, F. Yesilcimen, A. Aslan, Biosorption of heavy metal from aqueous solution by dried lichens, Int. J. Chem. 11 (2001) 141–146.
[41] R. Watkins, D. Weiss, W. Dubbin, K. Peel, B. Coles, T. Arnold, Investigations into the kinetics and thermodynamics of Sb(III) adsorption on goethite (α-FeOOH), J. Colloid Interface Sci. 303 (2006) 639–646.
[42] Y.-H. Xu, A. Ohki, S. Maeda, Adsorption and removal of antimony from aqueous soluiotn by an activated alumina 1. Adsorption capacity of adsorbent and effect of process variable, Toxicol. Environ. Chem. 80 (2001) 133–144.
[43] A. Sari, D. Mendil, M. Tuzen, M. Soylak, Biosorption of Cd(II) and Cr(III) from aqueous solution by moss (*Hylocomium splendens*) biomass: equilibrium, kinetic and thermodynamic studies, Chem. Eng. J. 144 (2008) 1–9.
[44] R. Altun Anayurt, A. Sari, M. Tuzen, Equilibrium, thermodynamic and kinetic studies on biosorption of Pb(II) and Cd(II) from aqueous solution by macrofungus (*Lactarius scrobiculatus*) biomass, Chem. Eng. J. 151 (2009) 255–261.
[45] M. Tuzen, A. Sari, Biosorption of selenium from aqueous solution by green algae (*Cladophora hutchinsiae*) biomass: equilibrium, thermodynamic and kinetic studies, Chem. Eng. J. 158 (2010) 200–206.
[46] K.P. Yadav, B.S. Tyagi, Fly-ash for the treatment of Cd-rich effluent, Environ. Technol. Lett. 8 (1987) 225–234.
[47] I. Langmuir, The adsorption of gases on plane surfaces of glass, mica and platinium, J. Am. Chem. Soc. 40 (1918) 1361–1403.
[48] P. Thanabalasingam, W.F. Pickering, Specific sorption of antimony(III) by the hydrous oxides of Mn, Fe and Al, Water Air Soil Pollut. 49 (1990) 175–185.
[49] H.M.F. Freundlich, Über die adsorption in lösungen, Zeitschrift für Physikalische Chemie (Leipzig) 57A (1906) 385–470.
[50] M.M. Dubinin, E.D. Zaverina, L.V. Radushkevich, Sorption and structure of active carbons. I. Adsorption of organic vapors, Zhurnal Fizicheskoi Khimii 21 (1947) 1351–1362.
[51] F. Helfferich, Ion Exchange, McGraw Hill, NY, USA, 1962, p. 166.
[52] S. Lagergren, Zur theorie der sogenannten adsorption geloster stöffe, Kungliga Sevenska Vetenskapsakademiens, Handlingar 24 (1898) 1.
[53] Y.S. Ho, G. McKay, Pseudo-second order model for sorption processes, Process Biochem. 34 (1999) 451–465.
[54] Y.S. Ho, G. McKay, D.A.J. Wase, C.F. Forster, Study of the sorption of divalent metal ions on to peat, Ads. Sci. Technol. 18 (2000) 639–650.
[55] R.R. Sheha, E.A. El-Shazly, Kinetics and equilibrium modeling of Se(IV) removal from aqueous solutions using metal oxides, Chem. Eng. J. 160 (2010) 63–71.